# Coordinated Frequency Control of Flywheel Energy Storage and Diesel Generator in Amirkabir University of Technology (AUT) Microgrid

M. S. Mahdavi
*Electrical Engineering Department*
*Amirkabir University of Technology*
Tehran, Iran
msmahdavi@aut.ac.ir

Mehdi Bagheri
*Electrical and Computer Engineering Department*
*Nazarbayev University*
Nur-Sultan, Kazakhstan
mehdi.bagheri@nu.edu.kz

G. B. Gharehpetian
*Electrical Engineering Department*
*Amirkabir University of Technology*
Tehran, Iran
grptian@aut.ac.ir

***Abstract*— Diesel generator is considered as one of the most significant distributed generation units in microgrid which has commonly a governor system for frequency control. However, due to large time constant of its fuel injection system; its reaction in load variation is almost undesirable and sometimes causes noticeable frequency drop. In this study, a flywheel energy storage system (FESS) is introduced, studied and coordinated with a diesel generator emulator for frequency control in a real fabricated microgrid model. A new frequency control strategy is proposed for FESS based on the high-pass filtering. In this strategy, FESS compensates the high-frequency parts of the required power according to its speed, while the diesel generator provides other low-frequency parts. The simulation and experimental results demonstrate clearly the performance of the proposed strategy.**

***Keywords*— Flywheel energy storage, Frequency control, Microgrid, Diesel generator***

## I. INTRODUCTION

In microgrids, the role of energy storage devices is quite crucial. Battery energy storage system (BESSs), supercapacitors and FESSs are well-known energy storage systems used in microgrids. Energy storage systems are usually employed to keep and satisfy the frequency control as well as power compensation. The energy capacity of FESS is typically more than supercapacitor, and unlike the BESS, FESS has infinite lifetime approximately. In addition, the FESS is faster and its power injection capacity is larger than the BESS.

Till now, many control systems have been presented for FESS in different applications [1,2]. In [3], a new control strategy of FESS for power smoothing in wind power plant is presented. A study by [4] introduces a detailed control strategy for Machine-side (M-side) converter of flywheel, and field oriented control (FOC) is proposed for a coordinated control of FESS and wind turbine system. In a work by [5], a direct torque control (DTC) strategy for M-side converter of an induction-machine-based FESS coordinated with a wind turbine for its output power smoothing is discussed, while [6] offers a new control system for PV output power smoothing by FESS.

Implementation of FESS for frequency regulation of microgrids has been studied in many literatures. For instance, in [7] a frequency control strategy for FESS, in a diesel-generator-based microgrid, by fuzzy PI controllers, is presented. In the same study, the FESS is responsible for frequency control. The coordination of FESS and diesel generator is neglected while it is known that the energy of FESS is limited and its power injection in primary control must be supported by an energy source like diesel generator in secondary control.

In [8], another frequency control system of FESS in a microgrid including fuel cell, PV and diesel generator is discussed. Also, the FESS is considered as the main frequency controller of the microgrid, while the coordination of FESS and the governor system of the diesel generator is neglected. The same problem can be found in [9], while in [10] a frequency regulation system for a combined system of wind power generation and FESS is highlighted and discussed. The machine type of FESS is called PMSM. Its M-side c utilizes a simple current control system. A fuzzy system is used to tune the PD-based frequency controller which generates the d-axis reference current for current controllers. The defects of this system, are very high cost of PMSM and probable instability due to the treatment of simple current control loops in FESS control system. Also in [10], FESS is supposed to be the main frequency controller of the grid which is possible just for primary control. Unfortunately, the paper does not clear the coordination of the FESS with other energy resources in secondary control.

In our study, a new frequency control system is proposed for FESS in coordination with diesel generator in microgrid. Considering two operation modes of FESS including speed control and frequency control modes; the proposed control system is a combination of both control strategies as the output of frequency control mode is the speed reference. Therefore, the FESS can automatically be recharged after each frequency compensation period. Also the proposed control system has an adaptive high-pass filter; thus, the FESS compensates the high frequency parts of the required power according to its speed while the diesel generator provides other low frequency parts. Moreover, a fourth-order Butterworth high-pass filter is presented and compared with

978-1-7281-0653-3/19/$31.00 ©2019 IEEE

first-order high-pass filter. In section II, a fabricated microgrid model at AUT microgrid and its different parts are introduced. In section III, the proposed control system of FESS, is presented. In section IV, the adaptive Butterworth filter is discussed and Section V provides simulation and experimental results following with Conclusion in Section VI.

## II. AUT MICROGRID

The diagram of AUT microgrid has been illustrated in Fig. 1. This microgrid model consists of four different modules including: (i.) Generator unit in the form of diesel generator emulator (DGE), (ii.) Programmable load unit in the form of load emulator, (iii.) Energy storage unit in the form of FESS and (iv.) constant resistive load.

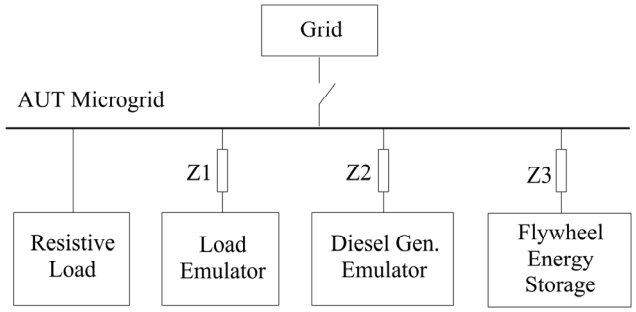


Fig. 1. Diagram of AUT microgrid

### A. Diesel Generator Emulator

The detailed structure and control system of DGE have been previously presented in [11]. As shown in Fig. 2, this control system consists of a three-phase rectifier, a DC link capacitor, an inverter and output LC filter. The output of inverter is connected to the microgrid. DGE can emulate the behavior of a real diesel generator including the governor system, fuel injection system, diesel engine model, AVR and synchronous machine model, with more control flexibility.

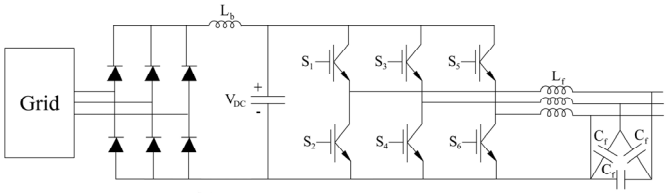


Fig. 2. Diesel generator emulator topology

Due to the large time constant of fuel injection system of diesel generator, its low speed power injection against the load change, will relatively lead to more frequency variations. This problem can be addressed using an energy storage system with fast power injection competence, like FESS.

### B. Load Emulator

The detailed structure and control system of load emulator previously have been presented in [12]. As shown in Fig. 3, it consists of an inverter-based rectifier and a buck converter with a resistive load in its output. It can play the role of a programmable PQ load and sink the pre-determined active and reactive power profiles such as step load or periodic triangular and sinusoidal power waveforms. It can be utilized for frequency control study in different load change scenarios.

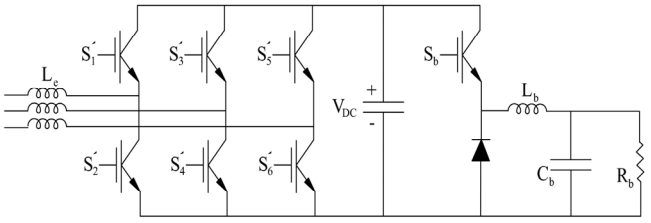


Fig. 3 Load emulator topology

### C. FESS

It is clear in Fig. 4 that the FESS structure consists of two back-to-back converters, including a grid-side (G-side) converter and an M-side converter which is connected to an IM. The shaft of the IM is connected to a massive cylinder with high momentum of inertia called as "flywheel". For the aim of frequency regulation, when the total generation is more than the total load, the IM is driven as a motor to absorb the extra power and prevent the frequency increasing. Once the total load is more than total generation, IM is driven as a generator to inject the required power and prevent the frequency drop. The proposed control strategies of G-side and M-side converters of FESS are presented in the next section.

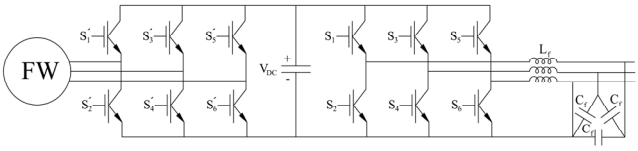


Fig. 4. Flywheel energy storage system topology

### D. Induction machine model

The voltage ($v$), current ($i$) and flux ($\lambda$) of rotor (index $r$) and stator (index $s$) of an induction machine in $dq$ frame can be written as follows:

$$\begin{aligned}\frac{d}{dt}\begin{bmatrix}\lambda_{sd}\\ \lambda_{sq}\end{bmatrix} &= \begin{bmatrix}v_{sd}\\ v_{sq}\end{bmatrix} - R_s\begin{bmatrix}i_{sd}\\ i_{sq}\end{bmatrix} - \omega_s\begin{bmatrix}0 & -1\\ 1 & 0\end{bmatrix}\begin{bmatrix}\lambda_{sd}\\ \lambda_{sq}\end{bmatrix}\\ \frac{d}{dt}\begin{bmatrix}\lambda_{rd}\\ \lambda_{rq}\end{bmatrix} &= \begin{bmatrix}v_{rd}\\ v_{rq}\end{bmatrix} - R_r\begin{bmatrix}i_{rd}\\ i_{rq}\end{bmatrix} - \omega_r\begin{bmatrix}0 & -1\\ 1 & 0\end{bmatrix}\begin{bmatrix}\lambda_{rd}\\ \lambda_{rq}\end{bmatrix}\end{aligned} \quad (1)$$

where $\omega_s$ and $\omega_r$ are electrical angular speed of rotor and stator flux. The relation of $\omega_s$ and $\omega_r$ is obtained by,

$$\omega_r = \omega_s - \frac{P}{2}\omega_{mech} \quad (2)$$

where $\omega_{mech}$ is the mechanical speed of rotor. The relation of fluxes and currents can be given as (3) based on the stator, rotor and mutual inductances (respectively *Ls*, *Lr* and *Lm*),

$$\begin{bmatrix}\lambda_{sd}\\ \lambda_{sq}\\ \lambda_{rd}\\ \lambda_{rq}\end{bmatrix}=\begin{bmatrix}L_s & 0 & L_m & 0\\ 0 & L_s & 0 & L_m\\ L_m & 0 & L_s & 0\\ 0 & L_m & 0 & L_s\end{bmatrix}\begin{bmatrix}i_{sd}\\ i_{sq}\\ i_{rd}\\ i_{rq}\end{bmatrix} \quad (3)$$

where,

$$L_s = L_{ls} + L_m$$
$$L_r = L_{lr} + L_m \quad (4)$$

Also the electrical torque of the shaft can be calculated as,

$$T_e = \frac{P}{2}(\lambda_{rq} i_{rd} - \lambda_{rd} i_{rq}) \quad (5)$$

where $P$ is the poles' number. On the other hand, newton's law in rotational form, can be written as follows (where $D$ is the damper coefficient),

$$J\frac{d\omega_{mech}}{dt} + D\omega_{mech} = T_e - T_{mech} \quad (6)$$

The required energy value of FESS ($E_{FW}$) must be considered for the design of $J$ according to (7).

$$E_{FW} = \frac{1}{2}J(\omega_{FW,\max}^2 - \omega_{FW,\min}^2) \quad (7)$$

where $\omega_{FW,\max}$ and $\omega_{FW,\max}$ are maximum and minimum of safe operation speed of FESS respectively. According to above equations, the model of IM for FESS can be presented as the block diagram in Fig. 5. M and H are both constant matrixes in (1) and (3) respectively.

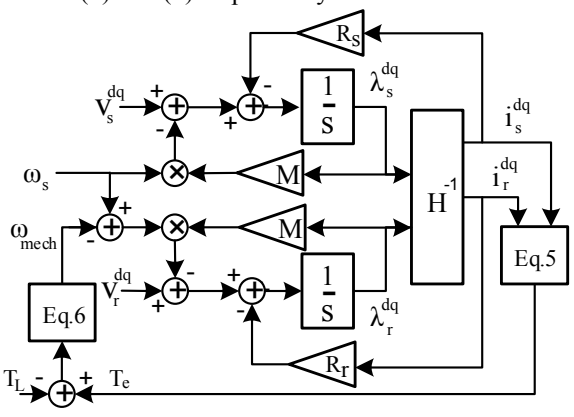


Fig. 5. Induction machine model of FESS

In this model, the mechanical torque ($T_L$) and $v_r^{dq}$ are equal to zero.

## III. Proposed Control Strategy for FESS

As shown in Fig. 4 and also discussed earlier, FESS has two back-to-back converters and operates in two modes including:

- Speed control mode
- Frequency control mode

In speed control mode, the control system tries to set the speed of flywheel to a reference value. Once the FESS is connected to the microgrid, it operates in speed control mode with a ramp speed reference and slowly is charged by power absorption as a motor, when the flywheel is reached to its rated speed, the control mode will change then to frequency control mode. In this section, at first the conventional G-side converter control and speed control mode of M-side converter are explained, and then the proposed frequency control mode for M-side converter is discussed by introducing two kinds of high-pass filters.

### *A. G-side converter control*

The conventional control method for G-side converter is shown in Fig. 6. The G-side converter controls the DC bus voltage by two cascaded PI controllers in d-axis and reactive power injection to the grid by two cascaded PI controllers in q-axis. The first PI controller in d-axis regulates the common DC bus voltage and generates the reference of $i_d$ for the next stage. The second PI controller in d-axis, is a current controller in order to track the reference of $i_d$ and generate the d-axis part of the reference voltage for PWM switching. The similar system is employed in q-axis for the reactive power reference tracking.

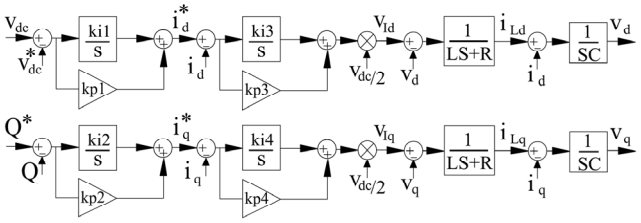


Fig. 6. G-side converter of FESS and its control system

### *B. Speed control mode for M-side converter*

The conventional speed mode control for M-side converter, is shown in Fig. 7, based on FOC. The M-side converter controls the flywheel speed ($\omega$) by three cascaded PI controllers in d-axis. Also it controls the rotor flux of IM by two cascaded PI controllers in q-axis. The first PI controller in d-axis, regulates the speed and generates the reference of the torque for the next stage. The second PI controller in d-axis will track the reference torque and generate the reference of $i_d$. The third PI controller is a current controller in order to track the reference of $i_d$ and generate the d-axis part of reference voltage for PWM switching. The similar system is used in q-axis for the rotor flux reference tracking. The estimator unit estimates the torque and rotor flux according to the measured stator currents.

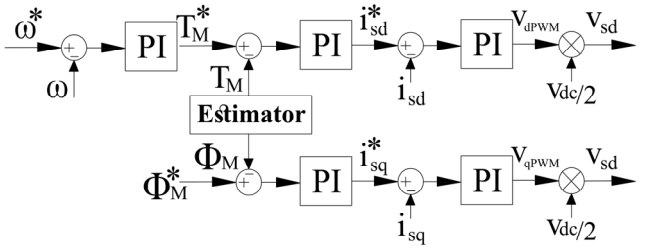


Fig. 7. M-side converter of FESS and its control system in speed control mode

### C. Proposed frequency control mode for M-side converter

In the frequency control mode, the control block of Fig. 8, is added to the control block of Fig. 7 to determine the reference of the speed according to the frequency regulation system. The measured frequency of the microgrid is compared with the reference value by a PI controller. The output of the PI controller passes through a high-pass filter (F(s)), and then the output is subtracted from the rated speed of the flywheel to generate the new speed reference. This strategy resolves the problem of changing the mode from "speed control mode" to "frequency control mode". Also the FESS can automatically be recharged after each frequency compensation period.

The proposed F(s) filter supports the FESS and diesel generator to coordinate together in frequency control. The high-pass filter causes that the FESS just compensates the power swings. Therefore, the DC term and low-frequency terms of the required power, are provided by the diesel generator.

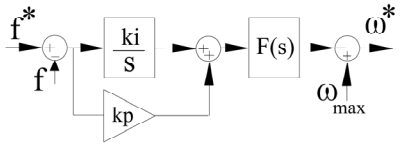


Fig. 8. The proposed frequency control system

The simplest form of high-pass filter is first-order high-pass filter with cutoff frequency of $\omega_c$. Also $n$-order Butterworth filter can be designed for more precision which is presented in the next section.

## IV. Adaptive Butterworth Filter

In this section, a Butterworth filter is presented and its adaptive form is utilized for frequency control in FESS. The magnitude of frequency response of an $n$-order Butterworth low-pass filter is given by,

$$|H(j\omega)| = \frac{1}{1+(\omega/\omega_C)^{2n}} \tag{8}$$

where $\omega_c$ is the cutoff frequency.

Considering upper and lower side of band width ( $A_{\min}$ in dB respected to $\omega_B$ and $A_{\max}$ in dB respected to $\omega_H$ ), the suitable order (n) can be designed as,

$$n = \frac{\log[(10^{0.1A_{\max}}-1)/(10^{0.1A_{\min}}-1)]}{2\log(\omega_H/\omega_B)} \tag{9}$$

Then $\omega_c$ can be determined by (10).

$$\omega_C = \frac{\omega_B}{\sqrt[2n]{10^{0.1A_{\min}}-1}} \tag{10}$$

Finally, the high-pass filter F(s) (illustrated in Fig. 8) is determined by,

$$F(s) = 1 - H(s) \tag{11}$$

In the proposed adaptive form of Butterworth filter for FESS, $\omega_c$ is determined according to the speed of the flywheel or in other words, the state of charge (SoC) of the flywheel. The lower $\omega_c$ means more FESS power injection and contribution against the load changes and frequency variations. Therefore in adaptive frequency control system of FESS, $\omega_c$ can be determined according to the on-line measured value of flywheel speed ($\omega_{FW}$) as follows:

$$\omega_c = \frac{2\pi\times10\times(\omega_{FW,\max}-\omega_{FW,\min})}{\omega_{FW}-\omega_{FW,\min}} \tag{12}$$

According to (12), if $\omega_{FW} = \omega_{FW,\max}$ then $\omega_c$ is equal to $2\pi\times10$ (its minimum value). It should be noted that the minimum value depends on the time constant of diesel generator in frequency control, specially the time constant of its fuel injection system.

## V. Experimental & Simulation Results

In this section, the experimental and simulation results of the proposed system are presented. AUT microgrid setup and its different parts (including load emulator, diesel generator emulator and FESS), can be found in Fig. 9. The system parameters for diesel generator, load emulator and FESS can be also found in [11], [12], [7] respectively.

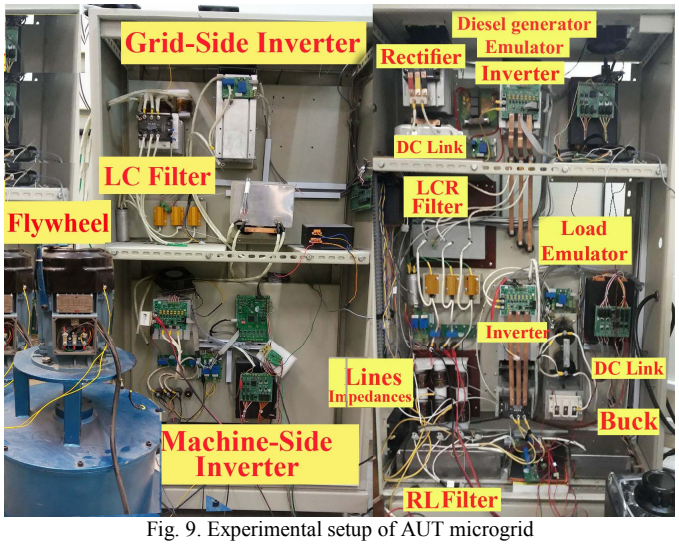


Fig. 9. Experimental setup of AUT microgrid

### A. Simulation results

According to the proposed models in sections II, III and IV, the detailed model-based simulation of microgrid is carried out by SIMULINK/MATLAB software, in three different scenarios including:

- In **Scenario 1**: a step change of load is applied by the load emulator, the diesel generator emulator is connected but the FESS is disconnected.
- In **Scenario 2**: a step change of load is applied by the load emulator, the diesel generator emulator and FESS are connected. The high-pass filter is a first-order filter.
- In **Scenario 3**: a step change of load is applied by the load emulator, the diesel generator emulator and FESS are connected. A 4th order Butterworth high-pass filter is used.

**Scenario 1:**

In this scenario, DGE is connected to resistive load and load emulator. At first, the reference of active and reactive power of load emulator is set to zero. In this form, DGE only provides 800W required power of resistive load. At t=12s, the reference of active power of load emulator will change to 1600W. As shown in Fig. 10, DGE responses to the load variation by its governor system. The frequency variation is depicted in Fig. 13 with the black color. It is clear that the high time constant of DGE leads to the relatively high frequency drops to 49.15Hz.

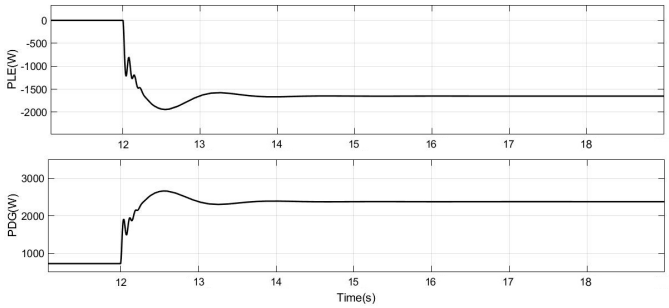


Fig. 10. Input power of Load emulator & output power of DGE in scenario 1

**Scenario 2:**

In this scenario, FESS is added to the previous scenario with the proposed control system with the assumption that F(s) is a first-order high-pass filter with $\omega_c = 2\pi \times 10$. At first, the reference of active and reactive power of load emulator is set to zero. Thus DGE only provides 800W which is required power of resistive load. At t=12s, the reference of active power of load emulator will change to 1600W.

As shown in Fig. 10, FESS is immediately compensates the existing power unbalancing (high-frequency parts of the required power) in about 2 seconds. Then DGE slowly responses to the low-frequency parts of the necessary power and the FESS output is reduced to be zero.

The frequency variation is depicted in Fig. 13 with the red color. Coordinated operation of FESS and DGE with the proposed method leads to the considerably less frequency drop in comparison to the previous scenario.

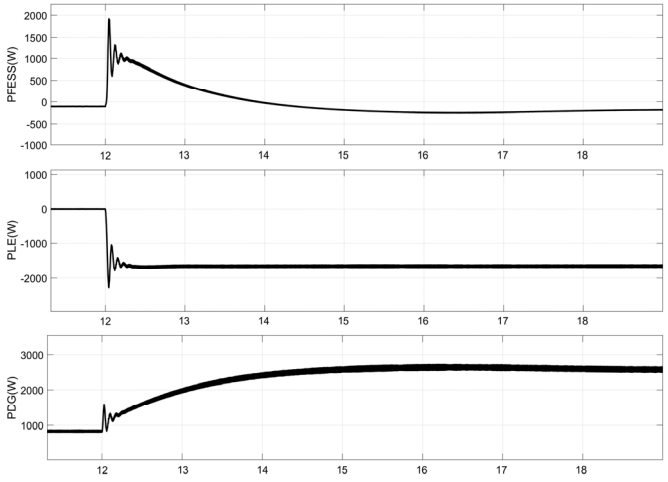


Fig. 11. Output power of FESS and DGE and input power of Load emulator in scenario 2

**Scenario 3:**

In this scenario, the proposed fourth-order Butterworth high-pass filter is used for F(s) in the frequency control system of FESS. Fig. 12 shows the power sharing among load emulator, DGE and FESS. The frequency variation of this scenario is depicted in Fig. 13 with the blue color. The proposed fourth-order Butterworth high-pass filter leads to the less frequency drops in comparison to the proposed first-order high-pass filter.

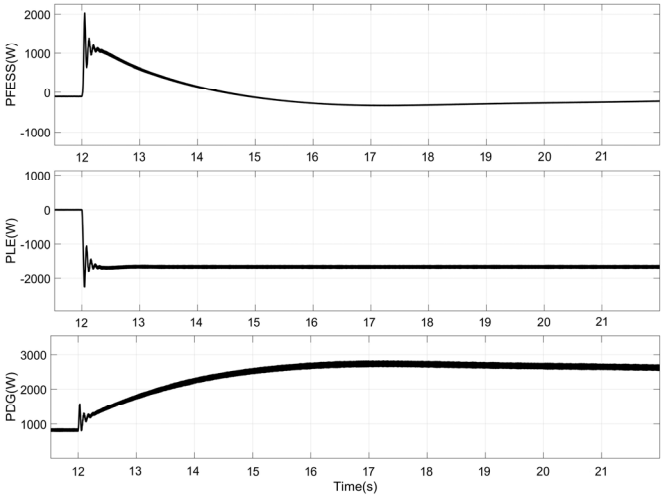


Fig. 12. Output power of FESS and DGE and input power of Load emulator in scenario 3

*B. Experimental results*

To verify the simulation results. The experimental results of the proposed method in AUT microgrid setup are presented in this section. The control systems are implemented on DSP microcontroller TMS320F28335 to generate the PWM pulses for drive circuits of IPMs. Also the discrete form of first-order high-pass filter and fourth-order Butterworth high-pass filter, are used in the digital control system with the sample rate of 10 kHz (Ts=0.0001s).

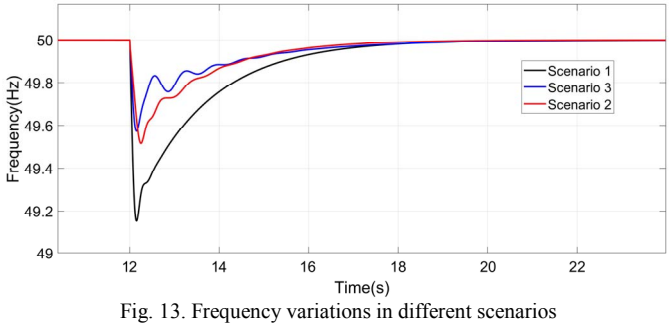


Fig. 13. Frequency variations in different scenarios

Fig. 14 shows the measured values of frequency in three mentioned scenarios. As it can be seen, the experimental results verify the simulation results. The coordinated frequency control of FESS with high-pass filtering method leads to reduce the frequency drop. The implemented digital

form of fourth-order Butterworth filter in DSP microcontroller, improves the frequency control in comparison to the digital form of 1st order high-pass filter.

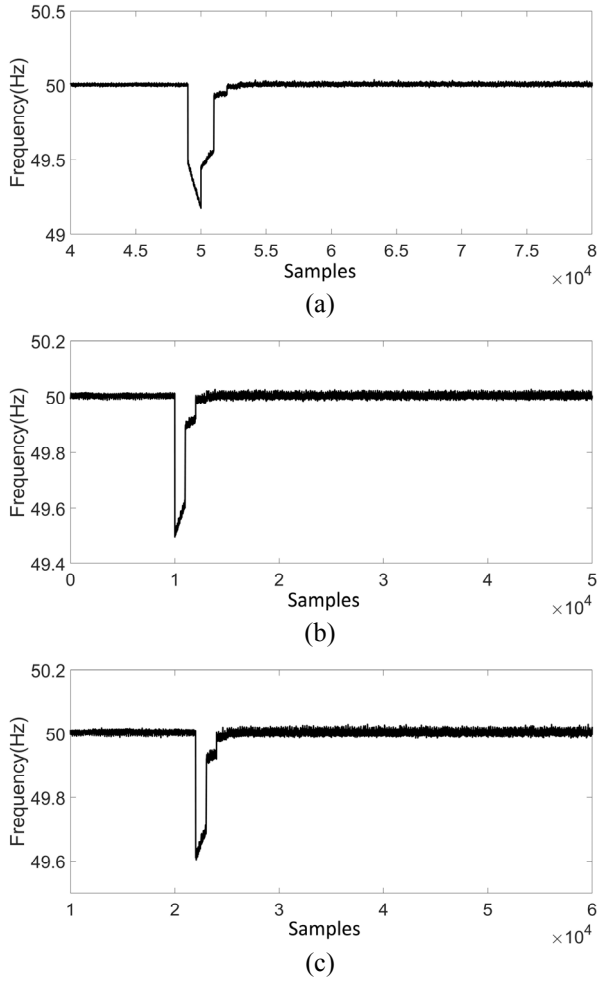


Fig. 14. Experimental variations of frequency against the step load change in (a) scenario 1, (b) scenario 2, (c) scenario 3

## VI. Conclusion

In this study, a new coordinated frequency control was proposed for FESS and also diesel generator in a real microgrid model. The proposed method was based on the high-pass filtering on the frequency control loop of M-side converter. Two types of high-pass filters were presented including the first-order high-pass filter and fourth-order Butterworth high-pass filter. In addition, an adaptive filtering approach was proposed to consider the SoC of FESS for unbalanced power compensation. The simulation and experimental results in AUT microgrid setup revealed that the FESS can supports the diesel generator to considerably limit the frequency variations against the sudden load change by the high-pass filtering method. Also the fourth-order Butterworth filter exposed a better performance than first-order high-pass filter in terms of frequency drop magnitude value.

## References


[1] G. O. Suvire, M. G. Molina, and P. E. Mercado, "Improving the integration of wind power generation into AC microgrids using flywheel energy storage", IEEE Transactions on smart grid , Vol. 3, no. 4, pp. 1945-1954, 2012.

[2] G. O. Suvire, Leonardo J. Ontiveros, and P. E. Mercado, "Combined control of a flywheel energy storage system and a vanadium redox flow battery for wind energy applications in microgrids", Dyna Vol. 84, no. 202, pp. 230-238, 2017.

[3] F. Diaz-Gonzalez, F. B. Bianci, A. sumper and O. Gomis-Bellmunt, "Control of a flywheel energy storage system for power smoothing in wind power plants", IEEE Transactions on Energy Conversion Vol. 29, no. 1, pp. 204-214, 2014.

[4] G. Cimuca, S. Breban and M. M. Radulescu, "Design and control strategies of an induction-machine-based flywheel energy storage system associated to a variable-speed wind generator", IEEE Transactions on Energy Conversion, Vol. 25, no. 2, pp. 526-534, 2010.

[5] M. Mansour, S. Rachdi, M. N. Mansouri, and M. F. Mimouni, "Direct torque control strategy of an induction-machine-based Flywheel energy storage system associated to a variable-speed wind generator" Energy and Power Engineering, Vol. 4, no. 4, pp. 255, 2012.

[6] A. Awad and I. Tumar ,"PV output power smoothing using flywheel storage system" 2017 IEEE International Conference on Environment and Electrical Engineering and 2017 IEEE Industrial and Commercial Power Systems Europe (EEEIC/I&CPS Europe). IEEE, 2017.

[7] M. S. Mahdavi, G. B. Gharehpetian, P. Ranjbaran, and H. Azizi, "Frequency regulation of AUT microgrid using modified fuzzy PI controller for flywheel energy storage system", In Power Electronics, Drives Systems and Technologies Conference (PEDSTC), 2018 9th Annual (pp. 426-431). IEEE, 2018.

[8] A. A. Khodadoost Arani, B. Zaker and G. B. Gharehpetian "Induction machine-based flywheel energy storage system modeling and control for frequency regulation after micro-grid islanding" International Transactions on Electrical Energy Systems, 27(9), e2356., 2017.

[9] Arani, AA Khodadoost, B. Zaker, and G. B. Gharehpetian. "A Control Strategy for Flywheel Energy Storage System for Frequency Stability Improvement in Islanded Microgrid" Iranian Journal of Electrical & Electronic Engineering, Vol. 13, no. 1, pp. 1-10, 2017.

[10] J. Yao, M. Yu, W. Gao and X. Zeng, "Frequency regulation control strategy for PMSG wind-power generation system with flywheel energy storage unit" IET Renewable Power Generation, Vol. 11, no. 8, pp. 1082-1093, 2016.

[11] M. S. Mahdavi, S. Ghasemi, H. Azizi and G. B. Gharehpetian, "design and implementation of a simple diesel generator emulator for frequency analysis in laboratory-scale microgrids" 2018 Smart Grid Conference (SGC). p. 1-6, IEEE, 2018.

[12] M. S. Mahdavi, G. B. Gharehpetian, P. Ranjbaran, and H. Azizi, "Fuzzy chopper-based load emulator for AUT microgrid", 2017 Smart Grid Conference (SGC). p. 1-6, IEEE, 2017.